POLITECNICO DI MILANO
DEPARTMENT OF ELECTRONICS, INFORMATION AND
BIOENGINEERING
DOCTORAL PROGRAMME IN COMPUTER SCIENCE

DEEP LEARNING FOR VISUAL STRUCTURED PREDICTION
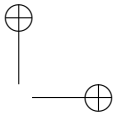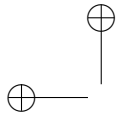
Doctoral Dissertation of:
Francesco Visin

Supervisor:
Prof. Matteo Matteucci

Co-Supervisor:
Prof. Aaron Courville
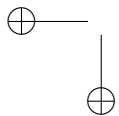
Tutor:
Prof. Andrea Bonarini

The Chair of the Doctoral Program:
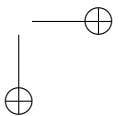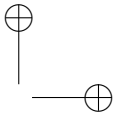**Prof. Coordinator Name**

2016 – XXVIII

All models are wrong, but some are useful.

GEORGE E. P. BOX
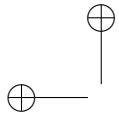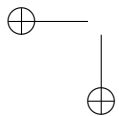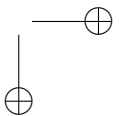
Abstract

A BSTRACT goes here.
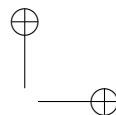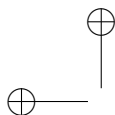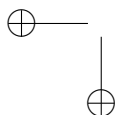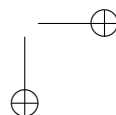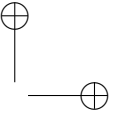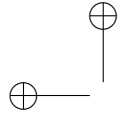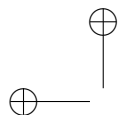
Summary

S UMMARY goes here.

Contents

Contents

CHAPTER 1

Introduction

1.1 Introduction

Or use `\footnote{That's a footnote}` like this[1]

1.2 New section

You can insert a definition

Definition 1.2.1. *PoliMi: Politecnico di Milano*

1.3 Another section

1.3.1 And a subsection

In this sub section I will include many images just to make the list of figures meaningful.

---

[1]That's a footnote

Chapter 1. Introduction

Figure 1.1: *Caption of this PoliMi image.*

1.4 New section

1.4.1 And also many sub

Or again more nested

- item 1

- item 2

- item 3

1.5 New section

This is an example of table. You can see it in Table 1.1.

Table 1.1: *Table caption*

Col 1	Col 2	Col2
Dim C.1	Dim C.3	Dim C.3
Data 1.1	Data 1.2	Data 1.3
Data 2.1	Data 2.2	Data 2.3
Data 3.1	Data 3.2	Data 3.3

1.6 You can do as many section as you want

The following equation has been created using $$: $y_1 = a * x + b$.

This is a more complex equation:

$$y_2 = a * x + b$$

, created using \[\]

This is, (1.1), an enumerated equation:

1.6. You can do as many section as you want

$$y_3 = a * x + b \qquad (1.1)$$

, created using:

```
\begin{equation}\label{eq:eeq1}
    y_3 = a*x + b
\end{equation}
```

CHAPTER *2*

Background

2.1 Introduction

Artificial intelligence (AI) is a broad field that aims to develop intelligent software that can e.g., acquire knowledge from its interaction with the world, find optimized strategies for problem solving, automate tasks, detect patterns in audio, video and textual data, play games, drive cars and much more.

Machine learning is a complex subfield of AI that witnessed a very quick expansion in the recent years. It aims to enable computers to *learn* how to tackle problems by detecting patterns and regularities in the training data and trying to generalize this extracted knowledge to new, unseen data.

Among its many powerful tools, artificial neural networks are models that take inspiration from what we know about the human brain, by mimicking its connectivity patterns, learning rules and signals propagation, under the constraints imposed by out limited knowledge of the brain and a less powerful hardware.

While it is beyond the scope of this document to give a formal and in-depth introduction to every concept needed to fully comprehend Machine Learning, the following sections will introduce Artificial neural networks, with a specific focus on two of the most used kinds of neural networks. For a detailed overview of Machine Learning, we suggest the interested reader to refer to Bishop (2006); Bengio and Courville (2016)

2.2 Artificial neural networks

Brains are composed by a large amount of simple elements, called neurons, that are highly interconnected. The number of neurons in the human brain is estimated to be around 10^{11}, each one connected to a little less than 10^4 other neurons, for a total between 10^{14} and 10^{15} synapses Drachman (2005). The activity of each of these either excites or inhibits the surrounding neurons it is connected to, generating a complex network of interactions.

Artificial Neural Networks (ANNs) take inspiration from this understanding of the human brain, building networks composed of many artificial neurons, small elements that perform very simple operations on their inputs.

2.2.1 Brief history of neural networks

In 1943 McCulloch and Pitts defined a mathematical model of how a biological neuron works (McCulloch and Pitts, 1943). The artificial neuron they proposed was able to solve simple binary problems, but did not learn. In 1949 Hebb (1949) suggested that human learn by enhancing the neural pathways between neurons that collaborate, and weakening the others. Only decades later this learning rule inspired the Perceptron (see Figure 2.1), the first ANN that was able to vary its own weights, i.e. to find the setting that allowed it to exhibit the desired behavior (Rosenblatt, 1957).

Figure 2.1: *A representation of the Perceptron.*

The activation rule of the perceptron is very simple and is at the base of many modern neural networks. Given an n-dimensional input x, the weighted sum of each dimension of the input x_i and its corresponding weight w_i – often referred to as *preactivation* – is computed as

$$z = \sum_{i=0}^{n} (w_i \cdot x_i)$$

where to simplify the notation the bias term b has been replaced by an equivalent input term $x_0 = b$. Note that this is simply the dot product of the weight matrix W, frequently referred to as *kernel*, and the input vector x. The result of this first affine transformation is then passed through a step function of form

$$y = \begin{cases} 1, & \text{if } z \geq 0 \\ 0, & \text{otherwise} \end{cases}$$

that determines the binary output of the Perceptron.

This can be used, e.g., to classify whether the input belongs to a specific class or not. Note that the model can be easily extended to handle multiple classes, by simply adding more dimensions to y and assigning each of them to a different class.

The behavior of the Perceptron is indeed remarkable, but the biggest innovation of Rosenblatt (1957) is most probably the update algorithm that allowed to modify the weights of the model in a Hebbian rule fashion. The weights and the bias – also called the *parameters* of the network – are *learned* according to the following rule:

$$w_i^{new} = w_i^{old} + \eta \cdot (\hat{y} - y) \cdot x_i \tag{2.1}$$

where $\hat{y}$ is the target (i.e. desired) value, y is the output of the Perceptron, x_i^t and w_i^t are respectively the i-th input and weight at time t and η is a scaling factor that allows to adjust the magnitude by which the weights are modified.

The introduction of a model that could learn from the data was welcomed with excitement as the beginning of a new era and research in ANNs became very active for approximately a decade, until in 1969 Minsky and Papert published a detailed mathematical analysis of the Perceptron, demonstrating that a single layered Perceptron could not model basic operations like the XOR logic operation (Minsky and Papert, 1969). The limit of Perceptrons is that they can only solve linearly separable problems, and fail at tackling nonlinearly separable problems like the XOR (see Figure 2.2). This is not the case for MultiLayer Perceptrons (MLP, depicted in Figure 2.3), an evolution of Perceptrons that introduces one or more intermediate layers (called *hidden layers*) between the input and the output. Since each of these layers is followed by a nonlinearity, the result is a nonlinear transformation that projects the input into a linearly separable space.

Figure 2.2: *a) A linearly separable problem. b) A nonlinearly separable problem. c) The XOR problem with a tentative solution that fails at separating the points of the space.*

The excessive enthusiasm for the early successes of ANNs turned into strong disappointment: even if Minsky and Papert (1969) showed that an MLP could model the XOR bitwise operation, it also pointed out that Rosenblatt's learning algorithm was limited to single layered Perceptrons and could not autonomously learn how to solve the problem. The expectation of an artificial intelligence that could learn by itself to solve problems and

Chapter 2. Background

interact with humans appeared suddenly unrealistic and most of the research community lost interest in ANNs. The field experienced a severe slow down and most of the fundings were cut.

After a decade known as the AI Winter, in 1982 John Hopfield presented a model of the human memory that did not only give insights on how the brain works, but was also useful in practical applications and had a sound and detail mathematical grounding. At the same time at the US-Japan Joint Conference on Cooperative/Competitive Neural Networks Japan announced a renewed effort in building Neural Networks and the fear that the US might be left behind renewed their effort on this topic.

The breakthrough that completely restored the interest in the field came in 1986, when Rumelhart *et al.* (1986) rediscovered the backpropagation algorithm (Linnainmaa, 1970; Werbos, 1974) that allowed to train ANNs composed by multiple layers by performing gradient descent (see Section 2.2.4). Since then ANNs have been constantly focus of study and innovation and established the state of the art in several domains.

2.2.2 MultiLayer Perceptron

Figure 2.3: *A MultiLayer Perceptron. The sum and the nonlinearity nodes have been omitted for the sake of clarity.*

Consider the network in Figure 2.3. As opposed to the Perceptron, the MLP has multiple hidden layers, where each neuron of one hidden layer is connected to all the neurons of the previous and next layer. Each connection from a neuron i to a neuron j in layer l is associated to a weight $w_{ij}^{(l)}$. Similarly to the Perceptron case, each layer computes an affine transformation, followed by a nonlinearity that is usually called *activation function*.

The processing performed by the hierarchy of layers of the MLP is equivalent to a composition of multiple functions

$$y = h_\theta^{(L)} \circ h_\theta^{(L-1)} \circ \cdots \circ h_\theta^{(1)} \tag{2.2}$$

Each of these functions $h^{(l)}$ depends on some parameters - namely the weights and bias of the layer, $W^{(l)}$ and $b^{(l)}$, as well as the choice of activation function for the layer $a^{(l)}$. It

is common to refer to the parameters that fully characterize a layer as *sufficient statistics*, usually denoted as θ.

The MLP is not the only architecture used in ANNs. In **??** two of the most used alternatives will be described. In general every layer of an ANN will compute some activation based on its input and a nonlinearity, that is usually different from the one proposed in the Perceptron paper. In the following section, some of the most used activation functions will be described.

2.2.3 Activation functions

Figure 2.4: *Some of the most common activation functions: sigmoid, tanh, ReLU and Leaky ReLU*

The activation function is one of the most important component of an ANN. As explained in the previous sections, to tackle nonlinearly separable problems it is imperative to map the input into a space that is linearly separable. The activation function does this by performing an *element-wise nonlinear transformation* of the pre-activation that comes from the affine transformation.

The affine transformation and the nonlinearity work together in a very tight interaction: the latter is fixed and does not evolve during training, but is a powerful transformation; the former instead, is determined by the weights that are learned during training and exploits the latter to map the incoming activation into a new space where they are easier to separate.

In addition to this it is interesting to point out that if there was no activation function, since the composition of multiple affine transformation is an affine transformation, the layers of the MLP could be replaced by a single equivalent layer, and the MLP would become a Perceptron.

Many activation functions have been proposed in the years and even if our understanding of this component has improved, which one to use with the different architectures and tasks is still object of active debate and a matter of personal preference. The upcoming sections describe the ones that are most frequently used, in the context where the activation of the previous layer $l-1$ is defined as $a^{(l-1)}$ and the result of the affine transformation is denoted as $z^{(l)} = W^{(l)} \cdot a^{(l-1)}$.

Logistic

The logistic, often called *sigmoid*, is a differentiable monotonically increasing function that takes any real-valued number and maps it to $[0, 1]$. As evident from its representation in Figure 2.4, for large negative numbers it asymptotes to 0 while for large positive numbers it asymptotes to 1. It is defined as

$$\frac{1}{1 + \exp(-x)} \tag{2.3}$$

The logistic function has probably been the most used nonlinearity historically due to its possible interpretation as the firing rate of a neuron given its potential (i.e. the level of excitement provoked by its incoming spikes): when the potential is low the neuron fires less often whereas when the potential is high the frequency of the spikes increases.

Its use is not as widespread as it used to be though, due to two major drawbacks:

- *Saturation kills the gradient:* backpropagation Section 2.2.4 relies on the gradient of the error to determine the parameter update. The logistic function saturates at both ends, resulting in a very small or zero gradient. This problem – often referred to as *vanishing gradient* – makes training very slow or prevents it in some cases. This also makes the logistic units very sensitive to the initialization of the weights of the network, that ideally should be such that the initial input of the logistic function is close to zero.

- *The output is not zero-centered:* the dynamics of ANNs are usually complex and difficult to inspect, but it is widely believed that normalizing (i.e. zero-centered with unit variance) the intermediate activations of the network helps training (Ioffe and Szegedy (2015); Laurent *et al.* (2015); Arpit *et al.* (2016); Cooijmans *et al.* (2016)). The output of the logistic function is always positive, which causes the mean activation to be non-zero. This could introduce undesirable dynamics that could slow down or prevent training.

Hyperbolic tangent (tanh)

The hyperbolic tangent, typically shortened as *tanh*, is a differentiable monotonically increasing function that maps any real-valued number to $[-1, 1]$. This nonlinear function suffers from the same vanishing problem as the logistic, but its mean is centered in zero. Furthermore, the tanh is often chosen where it is desirable to be able to increase or decrease some quantity by small amounts, thanks to its codomain. It is defined as

$$\frac{1 - exp(-2x)}{1 + exp(-2x)} \tag{2.4}$$

Rectified Linear Unit (ReLU)

Since its introduction, the Rectified Linear Unit (ReLu) Jarrett *et al.* (2009); Nair and Hinton (2010) has become the nonlinearity of choice in many applications Krizhevsky *et al.* (2012a); LeCun *et al.* (2015); Anonymous (2010). Although very simple, it has some very interesting properties and a few drawbacks:

- *No positive saturation:* the ReLU is zero for non-positive inputs, but does not saturate otherwise. This ensures a flow of gradient whenever the input is positive that was found to significantly speed up the convergence of training.

- *Cheap to compute:* as opposed to many other activation functions that require expensive operations, such as e.g. exponentials, ReLU's implementation simply amounts to thresholding at zero. Another important characteristic is that the gradient is trivial to compute:

$$\nabla(ReLU) = \begin{cases} a^{(l-1)}, & \text{if } z^{(l)} > 0 \\ 0, & \text{if } z^{(l)} < 0 \\ undefined, & \text{if } z^{(l)} = 0 \end{cases}$$

- *Induce sparsity:* ReLU units induce sparsity, since whenever the input preactivation is negative their activation is zero. Sparsity is usually a desired property: as opposed to dense encoding, sparsity will produce representations where only a few entries will change upon small variations of the input, i.e. will produce a representation that is more consistent and robust to perturbations. Furthermore, sparsity allows for a more compact encoding, which is desirable in many contexts such as, e.g., data compression and efficient data transfer. Finally, it is also usually easier to linearly separate sparse representations (Glorot *et al.*, 2011).

- *ReLU units can die:* when a large gradient flows through a ReLU unit it can change its weights in such a way that will prevent it from ever being active again. In this case, the unit will always saturate on zero, this will prevent gradient flow and the unit will never leave this state becoming "dead". This can be alleviated using a lower learning rate or adopting some modification of ReLU less sensitive to this problem.

ReLU is defined as

$$max(0, x) \tag{2.5}$$

Leaky Rectified Linear Unit (Leaky ReLU)

Leaky ReLUs are one of the most adopted alternatives to ReLUs. They have been proposed as a way to alleviate the dying units problem of ReLUs, by preventing the unit from saturating allowing a small gradient to always flow through the unit, potentially recovering extreme values of the weights. Leaky ReLUs are defined as

$$max(\beta * x, x) \tag{2.6}$$

2.2.4 Backpropagation

The learning rule introduced with Perceptrons does not allow to train models with multiple layers (i.e. with *hidden* layers), such as the one depicted in Figure 2.3.

This is not possible due to the fact that to compute the variation of the weights of a layer with Equation 2.1 it is necessary to know the correct value of its output, which

Chapter 2. Background

is known only for the last layer. To address this apparently insurmountable obstacle it suffices to notice that the computation performed by the activation function is a nonlinear but differentiable function of the inputs. This allows for computing the partial derivatives of the error, i.e. the difference between the desired output and the actual one, w.r.t. the weights of the network. In other words, it is possible to use calculus to determine the amount by which each neuron of the last layer contributed to causing the error, and then further split the responsibility of each of them among the ones of the preceding layer. This way the error can be *backpropagated* through the layers of the network, assigning to each weight its amount of blame. This information can be used by an *optimization algorithm* to iteratively change the weights to minimize the error.

The backpropagation algorithm has some resemblance with the learning rule of the Perceptron (Equation 2.1). The main idea in that case was to modify each weight of the network by a factor proportional to the error $E = \hat{y} - y$ and to the input. Even if in MLP it is usually common to consider other kinds of errors, such as the mean squared error (MSE) $E_{MSE} = \frac{1}{n} \sum_{i=0}^{n} (\hat{y}_i - y_i)^2$, the same concept applies: the learning procedure tries to modify the weights in order to minimize the error.

The rest of this chapter will focus on two very common kinds of ANNs respectively characterized by a feedforward and feedback connectivity pattern, namely Convolutional Neural Networks and Recurrent Neural Networks.

2.3 Convolutional networks

Deep convolutional neural networks (CNNs) have been at the heart of spectacular advances in deep learning. Although CNNs have been used as early as the nineties to solve character recognition tasks (Le Cun *et al.*, 1997), their current widespread application is due to much more recent work, when a deep CNN was used to beat state-of-the-art in the ImageNet image classification challenge (Krizhevsky *et al.*, 2012b).

Convolutional neural networks therefore constitute a very useful tool for machine learning practitioners. However, learning to use CNNs for the first time is generally an intimidating experience. A convolutional layer's output shape is affected by the shape of its input as well as the choice of kernel shape, zero padding and strides, and the relationship between these properties is not trivial to infer. This contrasts with fully-connected layers, whose output size is independent of the input size. Additionally, CNNs also usually feature a *pooling* stage, adding yet another level of complexity with respect to fully-connected networks. Finally, so-called transposed convolutional layers (also known as fractionally strided convolutional layers) have been employed in more and more work as of late (Zeiler *et al.*, 2011; Zeiler and Fergus, 2014; Long *et al.*, 2015; Radford *et al.*, 2015; Visin *et al.*, 2015; Im *et al.*, 2016), and their relationship with convolutional layers has been explained with various degrees of clarity.

For an in-depth treatment of the subject, see Chapter 9 of the Deep Learning textbook (Bengio and Courville, 2016).

2.4 Discrete convolutions

The bread and butter of neural networks is *affine transformations*: a vector is received as input and is multiplied with a matrix to produce an output (to which a bias vector is

usually added before passing the result through a nonlinearity). This is applicable to any type of input, be it an image, a sound clip or an unordered collection of features: whatever their dimensionality, their representation can always be flattened into a vector before the transformation.

Images, sound clips and many other similar kinds of data have an intrinsic structure. More formally, they share these important properties:

- They are stored as multi-dimensional arrays.

- They feature one or more axes for which ordering matters (e.g., width and height axes for an image, time axis for a sound clip).

- One axis, called the channel axis, is used to access different views of the data (e.g., the red, green and blue channels of a color image, or the left and right channels of a stereo audio track).

These properties are not exploited when an affine transformation is applied; in fact, all the axes are treated in the same way and the topological information is not taken into account. Still, taking advantage of the implicit structure of the data may prove very handy in solving some tasks, like computer vision and speech recognition, and in these cases it would be best to preserve it. This is where discrete convolutions come into play.

A discrete convolution is a linear transformation that preserves this notion of ordering. It is sparse (only a few input units contribute to a given output unit) and reuses parameters (the same weights are applied to multiple locations in the input).

Figure 2.5 provides an example of a discrete convolution. The light blue grid is called the *input feature map*. To keep the drawing simple, a single input feature map is represented, but it is not uncommon to have multiple feature maps stacked one onto another.[1] A *kernel* (shaded area) of value

slides across the input feature map. At each location, the product between each element of the kernel and the input element it overlaps is computed and the results are summed up to obtain the output in the current location. The procedure can be repeated using different kernels to form as many output feature maps as desired (Figure 2.7). The final outputs of this procedure are called *output feature maps*.[2] If there are multiple input feature maps, the kernel will have to be 3-dimensional – or, equivalently each one of the feature maps will be convolved with a distinct kernel – and the resulting feature maps will be summed up elementwise to produce the output feature map.

---

[1] An example of this is what was referred to earlier as *channels* for images and sound clips.

[2] While there is a distinction between convolution and cross-correlation from a signal processing perspective, the two become interchangeable when the kernel is learned. For the sake of simplicity and to stay consistent with most of the machine learning literature, the term *convolution* will be used in this guide.

Chapter 2. Background
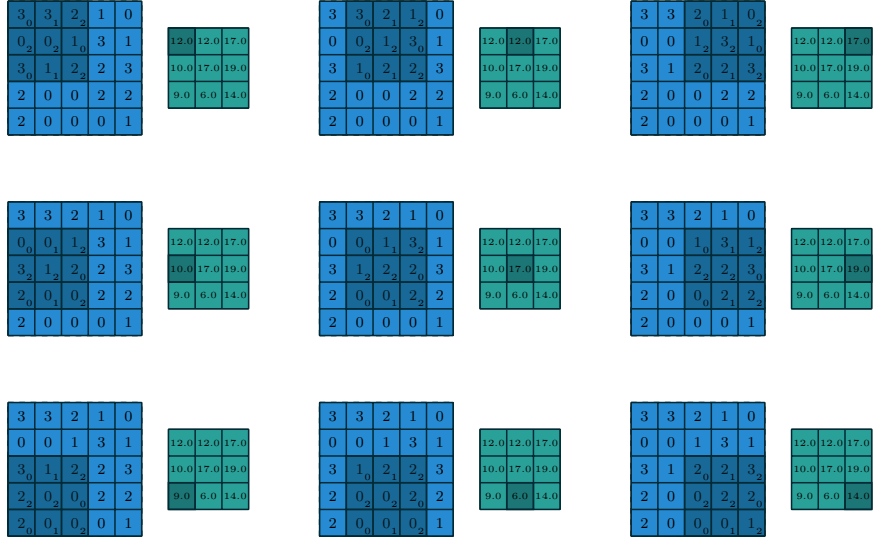

Figure 2.5: *Computing the output values of a discrete convolution.*
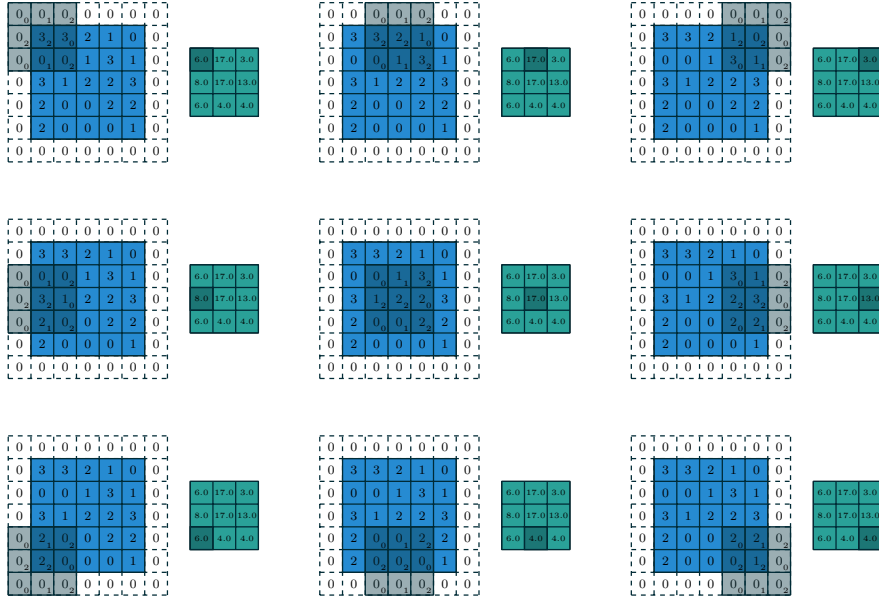

Figure 2.6: *Computing the output values of a discrete convolution for $N = 2$, $i_1 = i_2 = 5$, $k_1 = k_2 = 3$, $s_1 = s_2 = 2$, and $p_1 = p_2 = 1$.*

14

The convolution depicted in Figure 2.5 is an instance of a 2-D convolution, but it can be generalized to N-D convolutions. For instance, in a 3-D convolution, the kernel would be a *cuboid* and would slide across the height, width and depth of the input feature map.

The collection of kernels defining a discrete convolution has a shape corresponding to some permutation of $(n, m, k_1, \ldots, k_N)$, where

$$n \equiv \text{number of output feature maps,}$$
$$m \equiv \text{number of input feature maps,}$$
$$k_j \equiv \text{kernel size along axis } j.$$

The following properties affect the output size o_j of a convolutional layer along axis j:

- i_j: input size along axis j,

- k_j: kernel size along axis j,

- s_j: stride (distance between two consecutive positions of the kernel) along axis j,

- p_j: zero padding (number of zeros concatenated at the beginning and at the end of an axis) along axis j.

For instance, Figure 2.6 shows a 3×3 kernel applied to a 5×5 input padded with a 1×1 border of zeros using 2×2 strides.

Note that strides constitute a form of *subsampling*. As an alternative to being interpreted as a measure of how much the kernel is translated, strides can also be viewed as how much of the output is retained. For instance, moving the kernel by hops of two is equivalent to moving the kernel by hops of one but retaining only odd output elements (Figure 2.8).

2.5 Pooling

In addition to discrete convolutions themselves, *pooling* operations make up another important building block in CNNs. Pooling operations reduce the size of feature maps by using some function to summarize subregions, such as taking the average or the maximum value.

Pooling works by sliding a window across the input and feeding the content of the window to a *pooling function*. In some sense, pooling works very much like a discrete convolution, but replaces the linear combination described by the kernel with some other function. Figure 2.9 provides an example for average pooling, and Figure 2.10 does the same for max pooling.

The following properties affect the output size o_j of a pooling layer along axis j:

- i_j: input size along axis j,

- k_j: pooling window size along axis j,

- s_j: stride (distance between two consecutive positions of the pooling window) along axis j.
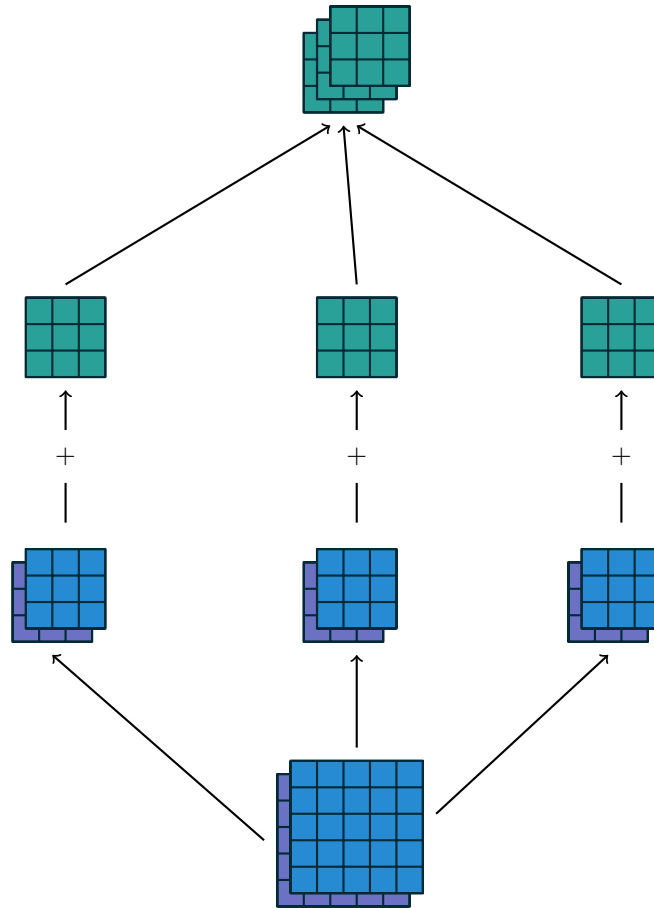
Chapter 2. Background

Figure 2.7: *A convolution mapping from two input feature maps to three output feature maps using a $3 \times 2 \times 3 \times 3$ collection of kernels $\mathbf{w}$. In the left pathway, input feature map 1 is convolved with kernel $\mathbf{w}_{1,1}$ and input feature map 2 is convolved with kernel $\mathbf{w}_{1,2}$, and the results are summed together elementwise to form the first output feature map. The same is repeated for the middle and right pathways to form the second and third feature maps, and all three output feature maps are grouped together to form the output.*
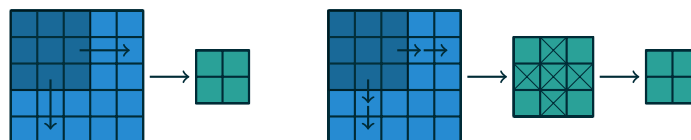

Figure 2.8: *An alternative way of viewing strides. Instead of translating the 3×3 kernel by increments of $s = 2$ (left), the kernel is translated by increments of 1 and only one in $s = 2$ output elements is retained (right).*
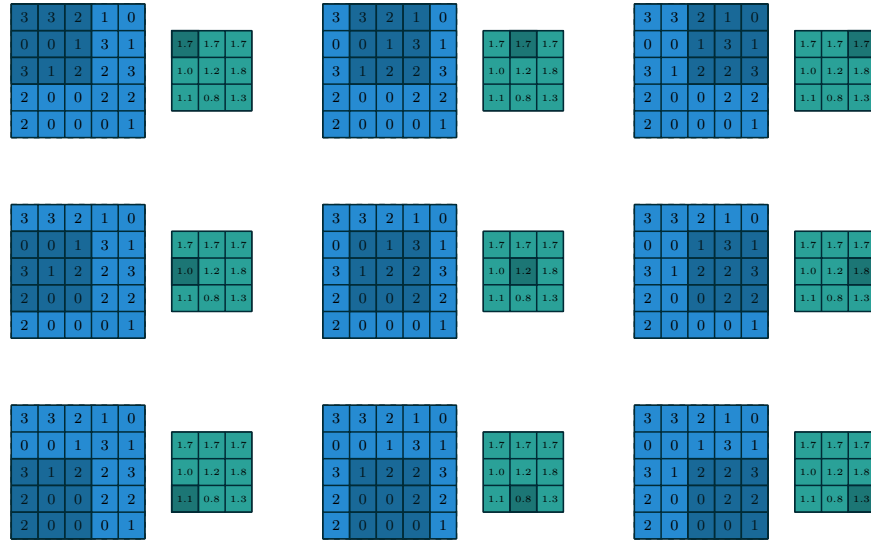
Figure 2.9: *Computing the output values of a 3×3 average pooling operation on a 5×5 input using 1×1 strides.*

Figure 2.10: *Computing the output values of a 3×3 max pooling operation on a 5×5 input using 1×1 strides.*
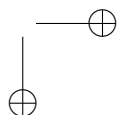
17

CHAPTER 3

Convolution arithmetic

The analysis of the relationship between convolutional layer properties is eased by the fact that they don't interact across axes, i.e., the choice of kernel size, stride and zero padding along axis j only affects the output size of axis j. Because of that, this chapter will focus on the following simplified setting:

- 2-D discrete convolutions ($N = 2$),

- square inputs ($i_1 = i_2 = i$),

- square kernel size ($k_1 = k_2 = k$),

- same strides along both axes ($s_1 = s_2 = s$),

- same zero padding along both axes ($p_1 = p_2 = p$).

This facilitates the analysis and the visualization, but keep in mind that the results outlined here also generalize to the N-D and non-square cases.

3.1 No zero padding, unit strides

The simplest case to analyze is when the kernel just slides across every position of the input (i.e., $s = 1$ and $p = 0$). Figure 3.1 provides an example for $i = 4$ and $k = 3$.

One way of defining the output size in this case is by the number of possible placements of the kernel on the input. Let's consider the width axis: the kernel starts on the leftmost

Chapter 3. Convolution arithmetic

part of the input feature map and slides by steps of one until it touches the right side of the input. The size of the output will be equal to the number of steps made, plus one, accounting for the initial position of the kernel (Figure 3.8a). The same logic applies for the height axis.

More formally, the following relationship can be inferred:

Relationship 1. *For any i and k, and for $s = 1$ and $p = 0$,*

$$o = (i - k) + 1.$$

3.2 Zero padding, unit strides

To factor in zero padding (i.e., only restricting to $s = 1$), let's consider its effect on the effective input size: padding with p zeros changes the effective input size from i to $i + 2p$. In the general case, Relationship 1 can then be used to infer the following relationship:

Relationship 2. *For any i, k and p, and for $s = 1$,*

$$o = (i - k) + 2p + 1.$$

Figure 3.2 provides an example for $i = 5$, $k = 4$ and $p = 2$.

In practice, two specific instances of zero padding are used quite extensively because of their respective properties. Let's discuss them in more detail.

3.2.1 Half (same) padding

Having the output size be the same as the input size (i.e., $o = i$) can be a desirable property:

Relationship 3. *For any i and for k odd ($k = 2n + 1, \quad n \in \mathbb{N}$), $s = 1$ and $p = \lfloor k/2 \rfloor = n$,*

$$
\begin{aligned}
o &= i + 2\lfloor k/2 \rfloor - (k - 1) \\
&= i + 2n - 2n \\
&= i.
\end{aligned}
$$

This is sometimes referred to as *half* (or *same*) padding. Figure 3.3 provides an example for $i = 5$, $k = 3$ and (therefore) $p = 1$.

3.2.2 Full padding

While convolving a kernel generally *decreases* the output size with respect to the input size, sometimes the opposite is required. This can be achieved with proper zero padding:
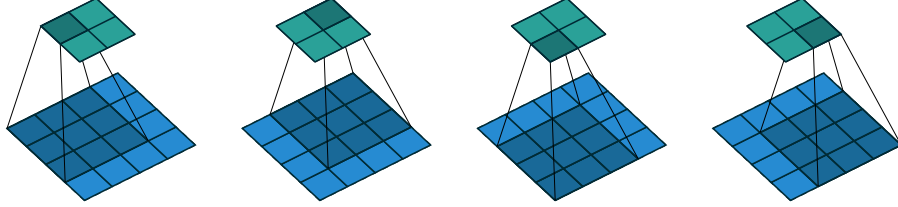
Figure 3.1: *(No padding, unit strides) Convolving a 3×3 kernel over a 4×4 input using unit strides (i.e., $i = 4$, $k = 3$, $s = 1$ and $p = 0$).*
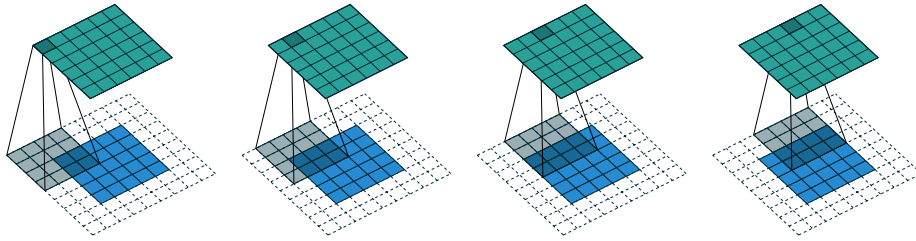

Figure 3.2: *(Arbitrary padding, unit strides) Convolving a 4×4 kernel over a 5×5 input padded with a 2×2 border of zeros using unit strides (i.e., $i = 5$, $k = 4$, $s = 1$ and $p = 2$).*

Figure 3.3: *(Half padding, unit strides) Convolving a 3×3 kernel over a 5×5 input using half padding and unit strides (i.e., $i = 5$, $k = 3$, $s = 1$ and $p = 1$).*

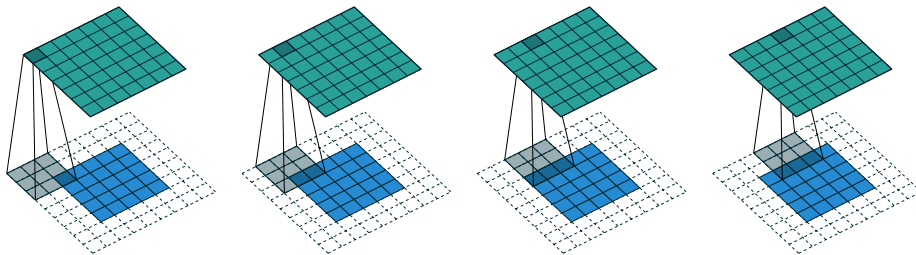**Figure 3.4:** *(Full padding, unit strides) Convolving a 3×3 kernel over a 5×5 input using full padding and unit strides (i.e., $i = 5$, $k = 3$, $s = 1$ and $p = 2$).*

Chapter 3. Convolution arithmetic

Relationship 4. *For any i and k, and for $p = k - 1$ and $s = 1$,*

$$o = i + 2(k - 1) - (k - 1)$$
$$= i + (k - 1).$$

This is sometimes referred to as *full* padding, because in this setting every possible partial or complete superimposition of the kernel on the input feature map is taken into account. Figure 3.4 provides an example for $i = 5$, $k = 3$ and (therefore) $p = 2$.

3.3 No zero padding, non-unit strides

All relationships derived so far only apply for unit-strided convolutions. Incorporating non unitary strides requires another inference leap. To facilitate the analysis, let's momentarily ignore zero padding (i.e., $s > 1$ and $p = 0$). Figure 3.5 provides an example for $i = 5$, $k = 3$ and $s = 2$.

Once again, the output size can be defined in terms of the number of possible placements of the kernel on the input. Let's consider the width axis: the kernel starts as usual on the leftmost part of the input, but this time it slides by steps of size s until it touches the right side of the input. The size of the output is again equal to the number of steps made, plus one, accounting for the initial position of the kernel (Figure 3.8b). The same logic applies for the height axis.

From this, the following relationship can be inferred:

Relationship 5. *For any i, k and s, and for $p = 0$,*

$$o = \left\lfloor \frac{i - k}{s} \right\rfloor + 1.$$

The floor function accounts for the fact that sometimes the last possible step does *not* coincide with the kernel reaching the end of the input, i.e., some input units are left out (see Figure 3.7 for an example of such a case).

3.4 Zero padding, non-unit strides

The most general case (convolving over a zero padded input using non-unit strides) can be derived by applying Relationship 5 on an effective input of size $i + 2p$, in analogy to what was done for Relationship 2:

Relationship 6. *For any i, k, p and s,*

$$o = \left\lfloor \frac{i + 2p - k}{s} \right\rfloor + 1.$$

As before, the floor function means that in some cases a convolution will produce the same output size for multiple input sizes. More specifically, if $i + 2p - k$ is a multiple of s, then

any input size $j = i + a, \quad a \in \{0, \ldots, s-1\}$ will produce the same output size. Note that this ambiguity applies only for $s > 1$.

Figure 3.6 shows an example with $i = 5$, $k = 3$, $s = 2$ and $p = 1$, while Figure 3.7 provides an example for $i = 6$, $k = 3$, $s = 2$ and $p = 1$. Interestingly, despite having different input sizes these convolutions share the same output size. While this doesn't affect the analysis for *convolutions*, this will complicate the analysis in the case of *transposed convolutions*.
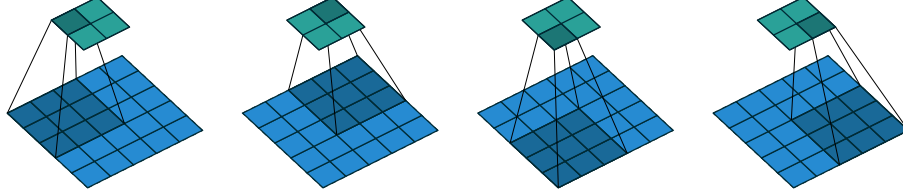
Chapter 3. Convolution arithmetic

Figure 3.5: *(No zero padding, arbitrary strides) Convolving a 3×3 kernel over a 5×5 input using 2×2 strides (i.e., $i = 5$, $k = 3$, $s = 2$ and $p = 0$).*

Figure 3.6: *(Arbitrary padding and strides) Convolving a 3×3 kernel over a 5×5 input padded with a 1×1 border of zeros using 2×2 strides (i.e., $i = 5$, $k = 3$, $s = 2$ and $p = 1$).*

Figure 3.7: *(Arbitrary padding and strides) Convolving a 3×3 kernel over a 6×6 input padded with a 1×1 border of zeros using 2×2 strides (i.e., $i = 6$, $k = 3$, $s = 2$ and $p = 1$). In this case, the bottom row and right column of the zero padded input are not covered by the kernel.*

(a) *The kernel has to slide two steps to the right to touch the right side of the input (and equivalently downwards). Adding one to account for the initial kernel position, the output size is 3×3.*

(b) *The kernel has to slide one step of size two to the right to touch the right side of the input (and equivalently downwards). Adding one to account for the initial kernel position, the output size is 2×2.*

Figure 3.8: *Counting kernel positions.*
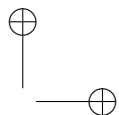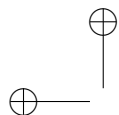
CHAPTER *4*

Pooling arithmetic

In a neural network, pooling layers provide invariance to small translations of the input. The most common kind of pooling is *max pooling*, which consists in splitting the input in (usually non-overlapping) patches and outputting the maximum value of each patch. Other kinds of pooling exist, e.g., mean or average pooling, which all share the same idea of aggregating the input locally by applying a nonlinearity to the content of some patches (Boureau *et al.*, 2010a,b, 2011; Saxe *et al.*, 2011).

Some readers may have noticed that the treatment of convolution arithmetic only relies on the assumption that some function is repeatedly applied onto subsets of the input. This means that the relationships derived in the previous chapter can be reused in the case of pooling arithmetic. Since pooling does not involve zero padding, the relationship describing the general case is as follows:
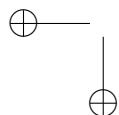
Relationship 7. *For any i, k and s,*

$$o = \left\lfloor \frac{i - k}{s} \right\rfloor + 1.$$
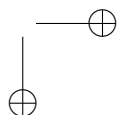
This relationship holds for any type of pooling.

CHAPTER 5

Transposed convolution arithmetic

The need for transposed convolutions generally arises from the desire to use a transformation going in the opposite direction of a normal convolution, i.e., from something that has the shape of the output of some convolution to something that has the shape of its input while maintaining a connectivity pattern that is compatible with said convolution. For instance, one might use such a transformation as the decoding layer of a convolutional autoencoder or to project feature maps to a higher-dimensional space.

Once again, the convolutional case is considerably more complex than the fully-connected case, which only requires to use a weight matrix whose shape has been transposed. However, since every convolution boils down to an efficient implementation of a matrix operation, the insights gained from the fully-connected case are useful in solving the convolutional case.

Like for convolution arithmetic, the dissertation about transposed convolution arithmetic is simplified by the fact that transposed convolution properties don't interact across axes.

The chapter will focus on the following setting:

- 2-D transposed convolutions ($N = 2$),

- square inputs ($i_1 = i_2 = i$),

- square kernel size ($k_1 = k_2 = k$),

- same strides along both axes ($s_1 = s_2 = s$),

Chapter 5. Transposed convolution arithmetic

- same zero padding along both axes ($p_1 = p_2 = p$).

Once again, the results outlined generalize to the N-D and non-square cases.

5.1 Convolution as a matrix operation

Take for example the convolution represented in Figure 3.1. If the input and output were to be unrolled into vectors from left to right, top to bottom, the convolution could be represented as a sparse matrix $\mathbf{C}$ where the non-zero elements are the elements $w_{i,j}$ of the kernel (with i and j being the row and column of the kernel respectively):

$$
\begin{pmatrix}
w_{0,0} & w_{0,1} & w_{0,2} & 0 & w_{1,0} & w_{1,1} & w_{1,2} & 0 & w_{2,0} & w_{2,1} & w_{2,2} & 0 & 0 & 0 & 0 & 0 \\
0 & w_{0,0} & w_{0,1} & w_{0,2} & 0 & w_{1,0} & w_{1,1} & w_{1,2} & 0 & w_{2,0} & w_{2,1} & w_{2,2} & 0 & 0 & 0 & 0 \\
0 & 0 & 0 & 0 & w_{0,0} & w_{0,1} & w_{0,2} & 0 & w_{1,0} & w_{1,1} & w_{1,2} & 0 & w_{2,0} & w_{2,1} & w_{2,2} & 0 \\
0 & 0 & 0 & 0 & 0 & w_{0,0} & w_{0,1} & w_{0,2} & 0 & w_{1,0} & w_{1,1} & w_{1,2} & 0 & w_{2,0} & w_{2,1} & w_{2,2}
\end{pmatrix}
$$

This linear operation takes the input matrix flattened as a 16-dimensional vector and produces a 4-dimensional vector that is later reshaped as the 2×2 output matrix.

Using this representation, the backward pass is easily obtained by transposing $\mathbf{C}$; in other words, the error is backpropagated by multiplying the loss with $\mathbf{C}^T$. This operation takes a 4-dimensional vector as input and produces a 16-dimensional vector as output, and its connectivity pattern is compatible with $\mathbf{C}$ by construction.

Notably, the kernel $\mathbf{w}$ defines both the matrices $\mathbf{C}$ and $\mathbf{C}^T$ used for the forward and backward passes.

5.2 Transposed convolution

Let's now consider what would be required to go the other way around, i.e., map from a 4-dimensional space to a 16-dimensional space, while keeping the connectivity pattern of the convolution depicted in Figure 3.1. This operation is known as a *transposed convolution*.

Transposed convolutions – also called *fractionally strided convolutions* – work by swapping the forward and backward passes of a convolution. One way to put it is to note that the kernel defines a convolution, but whether it's a direct convolution or a transposed convolution is determined by how the forward and backward passes are computed.

For instance, although the kernel $\mathbf{w}$ defines a convolution whose forward and backward passes are computed by multiplying with $\mathbf{C}$ and $\mathbf{C}^T$ respectively, it *also* defines a transposed convolution whose forward and backward passes are computed by multiplying with $\mathbf{C}^T$ and $(\mathbf{C}^T)^T = \mathbf{C}$ respectively.[1]

Finally note that it is always possible to emulate a transposed convolution with a direct convolution. The disadvantage is that it usually involves adding many columns and rows of zeros to the input, resulting in a much less efficient implementation.

Building on what has been introduced so far, this chapter will proceed somewhat backwards with respect to the convolution arithmetic chapter, deriving the properties of each transposed convolution by referring to the direct convolution with which it shares the kernel, and defining the equivalent direct convolution.

---

[1]The transposed convolution operation can be thought of as the gradient of *some* convolution with respect to its input, which is usually how transposed convolutions are implemented in practice.

5.3 No zero padding, unit strides, transposed

The simplest way to think about a transposed convolution is by computing the output shape of the direct convolution for a given input shape first, and then inverting the input and output shapes for the transposed convolution.

Let's consider the convolution of a 3×3 kernel on a 4×4 input with unitary stride and no padding (i.e., $i = 4$, $k = 3$, $s = 1$ and $p = 0$). As depicted in Figure 3.1, this produces a 2×2 output. The transpose of this convolution will then have an output of shape 4×4 when applied on a 2×2 input.

Another way to obtain the result of a transposed convolution is to apply an equivalent – but much less efficient – direct convolution. The example described so far could be tackled by convolving a 3×3 kernel over a 2×2 input padded with a 2×2 border of zeros using unit strides (i.e., $i' = 2$, $k' = k$, $s' = 1$ and $p' = 2$), as shown in Figure 5.1. Notably, the kernel's and stride's sizes remain the same, but the input of the transposed convolution is now zero padded.[2]

One way to understand the logic behind zero padding is to consider the connectivity pattern of the transposed convolution and use it to guide the design of the equivalent convolution. For example, the top left pixel of the input of the direct convolution only contribute to the top left pixel of the output, the top right pixel is only connected to the top right output pixel, and so on.

To maintain the same connectivity pattern in the equivalent convolution it is necessary to zero pad the input in such a way that the first (top-left) application of the kernel only touches the top-left pixel, i.e., the padding has to be equal to the size of the kernel minus one.

Proceeding in the same fashion it is possible to determine similar observations for the other elements of the image, giving rise to the following relationship:

Relationship 8. *A convolution described by $s = 1$, $p = 0$ and k has an associated transposed convolution described by $k' = k$, $s' = s$ and $p' = k - 1$ and its output size is*

$$o' = i' + (k - 1).$$

Interestingly, this corresponds to a fully padded convolution with unit strides.

5.4 Zero padding, unit strides, transposed

Knowing that the transpose of a non-padded convolution is equivalent to convolving a zero padded input, it would be reasonable to suppose that the transpose of a zero padded convolution is equivalent to convolving an input padded with *less* zeros.

It is indeed the case, as shown in Figure 5.2 for $i = 5$, $k = 4$ and $p = 2$.

Formally, the following relationship applies for zero padded convolutions:

---

[2]Note that although equivalent to applying the transposed matrix, this visualization adds a lot of zero multiplications in the form of zero padding. This is done here for illustration purposes, but it is inefficient, and software implementations will normally not perform the useless zero multiplications.

Chapter 5. Transposed convolution arithmetic

Relationship 9. *A convolution described by $s = 1$, k and p has an associated transposed convolution described by $k' = k$, $s' = s$ and $p' = k - p - 1$ and its output size is*

$$o' = i' + (k - 1) - 2p.$$

5.4.1 Half (same) padding, transposed

By applying the same inductive reasoning as before, it is reasonable to expect that the equivalent convolution of the transpose of a half padded convolution is itself a half padded convolution, given that the output size of a half padded convolution is the same as its input size. Thus the following relation applies:

Relationship 10. *A convolution described by $k = 2n + 1$, $n \in \mathbb{N}$, $s = 1$ and $p = \lfloor k/2 \rfloor = n$ has an associated transposed convolution described by $k' = k$, $s' = s$ and $p' = p$ and its output size is*

$$\begin{aligned} o' &= i' + (k - 1) - 2p \\ &= i' + 2n - 2n \\ &= i'. \end{aligned}$$

Figure 5.3 provides an example for $i = 5$, $k = 3$ and (therefore) $p = 1$.

5.4.2 Full padding, transposed

Knowing that the equivalent convolution of the transpose of a non-padded convolution involves full padding, it is unsurprising that the equivalent of the transpose of a fully padded convolution is a non-padded convolution:

Relationship 11. *A convolution described by $s = 1$, k and $p = k - 1$ has an associated transposed convolution described by $k' = k$, $s' = s$ and $p' = 0$ and its output size is*

$$\begin{aligned} o' &= i' + (k - 1) - 2p \\ &= i' - (k - 1) \end{aligned}$$

Figure 5.4 provides an example for $i = 5$, $k = 3$ and (therefore) $p = 2$.

5.5 No zero padding, non-unit strides, transposed

Using the same kind of inductive logic as for zero padded convolutions, one might expect that the transpose of a convolution with $s > 1$ involves an equivalent convolution with $s < 1$. As will be explained, this is a valid intuition, which is why transposed convolutions are sometimes called *fractionally strided convolutions*.
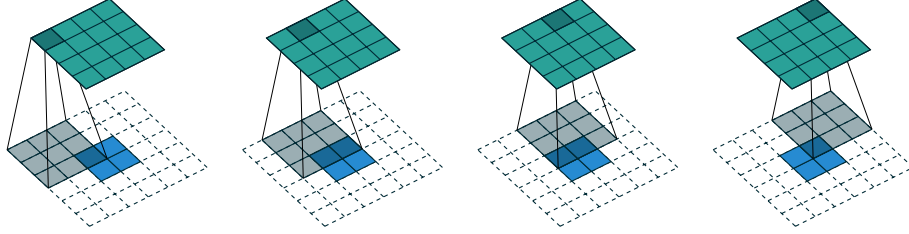
5.5. No zero padding, non-unit strides, transposed

Figure 5.1: *The transpose of convolving a 3×3 kernel over a 4×4 input using unit strides (i.e., $i = 4$, $k = 3$, $s = 1$ and $p = 0$). It is equivalent to convolving a 3×3 kernel over a 2×2 input padded with a 2×2 border of zeros using unit strides (i.e., $i' = 2$, $k' = k$, $s' = 1$ and $p' = 2$).*
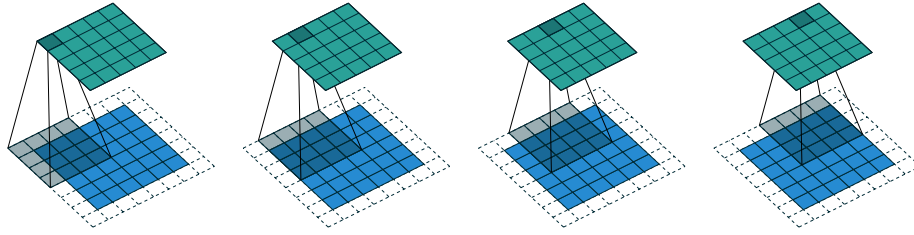

Figure 5.2: *The transpose of convolving a 4×4 kernel over a 5×5 input padded with a 2×2 border of zeros using unit strides (i.e., $i = 5$, $k = 4$, $s = 1$ and $p = 2$). It is equivalent to convolving a 4×4 kernel over a 6×6 input padded with a 1×1 border of zeros using unit strides (i.e., $i' = 6$, $k' = k$, $s' = 1$ and $p' = 1$).*

Figure 5.3: *The transpose of convolving a 3×3 kernel over a 5×5 input using half padding and unit strides (i.e., $i = 5$, $k = 3$, $s = 1$ and $p = 1$). It is equivalent to convolving a 3×3 kernel over a 5×5 input using half padding and unit strides (i.e., $i' = 5$, $k' = k$, $s' = 1$ and $p' = 1$).*

Chapter 5. Transposed convolution arithmetic

Figure 5.5 provides an example for $i = 5$, $k = 3$ and $s = 2$ which helps understand what fractional strides involve: zeros are inserted *between* input units, which makes the kernel move around at a slower pace than with unit strides.[3]

For the moment, it will be assumed that the convolution is non-padded ($p = 0$) and that its input size i is such that $i - k$ is a multiple of s. In that case, the following relationship holds:

Relationship 12. *A convolution described by $p = 0$, k and s and whose input size is such that $i - k$ is a multiple of s, has an associated transposed convolution described by $\tilde{i}'$, $k' = k$, $s' = 1$ and $p' = k - 1$, where $\tilde{i}'$ is the size of the stretched input obtained by adding $s - 1$ zeros between each input unit, and its output size is*

$$o' = s(i' - 1) + k.$$

5.6 Zero padding, non-unit strides, transposed

When the convolution's input size i is such that $i + 2p - k$ is a multiple of s, the analysis can extended to the zero padded case by combining Relationship 9 and Relationship 12:

Relationship 13. *A convolution described by k, s and p and whose input size i is such that $i + 2p - k$ is a multiple of s has an associated transposed convolution described by $\tilde{i}'$, $k' = k$, $s' = 1$ and $p' = k - p - 1$, where $\tilde{i}'$ is the size of the stretched input obtained by adding $s - 1$ zeros between each input unit, and its output size is*

$$o' = s(i' - 1) + k - 2p.$$

Figure 5.6 provides an example for $i = 5$, $k = 3$, $s = 2$ and $p = 1$.

The constraint on the size of the input i can be relaxed by introducing another parameter $a \in \{0, \ldots, s - 1\}$ that allows to distinguish between the s different cases that all lead to the same i':

Relationship 14. *A convolution described by k, s and p has an associated transposed convolution described by a, $\tilde{i}'$, $k' = k$, $s' = 1$ and $p' = k - p - 1$, where $\tilde{i}'$ is the size of the stretched input obtained by adding $s - 1$ zeros between each input unit, and $a = (i + 2p - k) \mod s$ represents the number of zeros added to the top and right edges of the input, and its output size is*

$$o' = s(i' - 1) + a + k - 2p.$$

Figure 5.7 provides an example for $i = 6$, $k = 3$, $s = 2$ and $p = 1$.

---

[3]Doing so is inefficient and real-world implementations avoid useless multiplications by zero, but conceptually it is how the transpose of a strided convolution can be thought of.
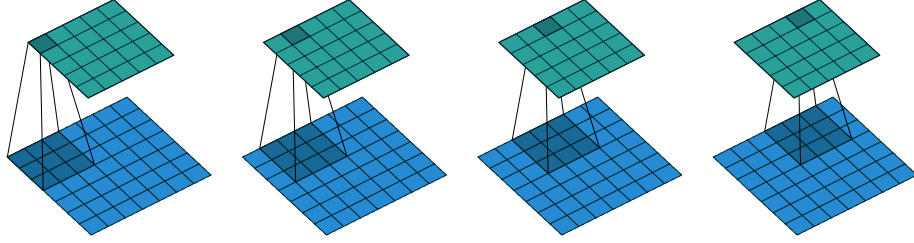
Figure 5.4: *The transpose of convolving a 3×3 kernel over a 5×5 input using full padding and unit strides (i.e., $i = 5$, $k = 3$, $s = 1$ and $p = 2$). It is equivalent to convolving a 3×3 kernel over a 7×7 input using unit strides (i.e., $i' = 7$, $k' = k$, $s' = 1$ and $p' = 0$).*
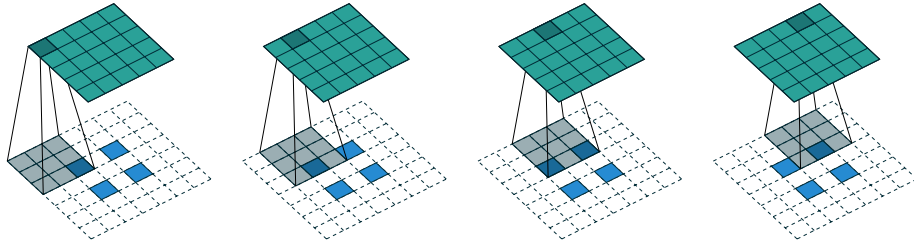

Figure 5.5: *The transpose of convolving a 3×3 kernel over a 5×5 input using 2×2 strides (i.e., $i = 5$, $k = 3$, $s = 2$ and $p = 0$). It is equivalent to convolving a 3×3 kernel over a 2×2 input (with 1 zero inserted between inputs) padded with a 2×2 border of zeros using unit strides (i.e., $i' = 2$, $\tilde{i}' = 3$, $k' = k$, $s' = 1$ and $p' = 2$).*
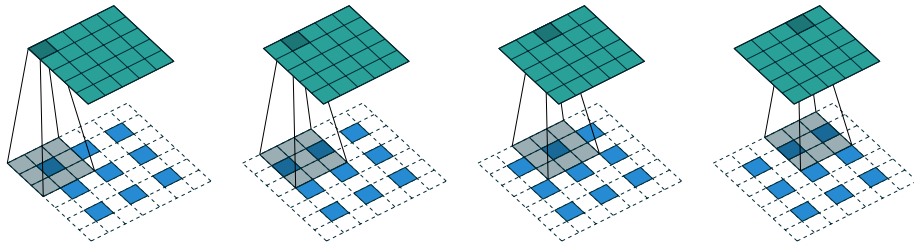
Figure 5.6: *The transpose of convolving a 3×3 kernel over a 5×5 input padded with a 1×1 border of zeros using 2×2 strides (i.e., $i = 5$, $k = 3$, $s = 2$ and $p = 1$). It is equivalent to convolving a 3×3 kernel over a 2×2 input (with 1 zero inserted between inputs) padded with a 1×1 border of zeros using unit strides (i.e., $i' = 3$, $\tilde{i}' = 5$, $k' = k$, $s' = 1$ and $p' = 1$).*

Chapter 5. Transposed convolution arithmetic

5.7 Recurrent networks

A biological neuron takes around 10^{-3} seconds to perform one operation, whereas a modern GPU can process up to NN DATA per second (**?**). Nonetheless, many tasks that are trivial for humans prove to be extremely complicated for computers. Why is that? The power of the brain lies in its large number of connections.**?**

It is well known that the brain is organized in functional areas, each of them usually structured in *layers* that process the incoming signal in an incremental fashion. These areas are usually connected both in a *feedforward*, i.e. to neurons belonging to deeper (i.e., further away from the input) layers, and in a *feedback* fashion (i.e. to previous layers in the hierarchy). Similarly, ANNs usually employ either feedforward or feedback connections.

Write something about RNNs, LSTMs, GRUs
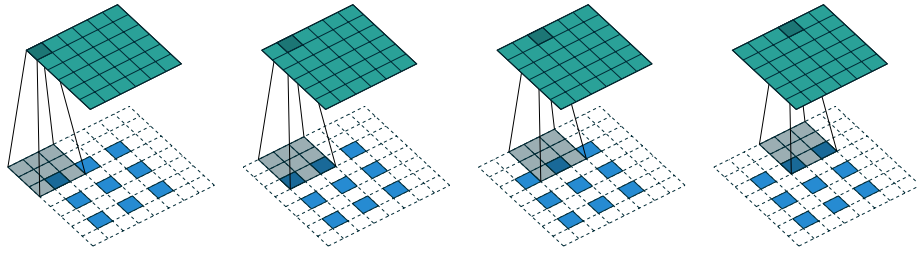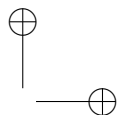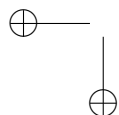
Figure 5.7: *The transpose of convolving a 3×3 kernel over a 6×6 input padded with a 1×1 border of zeros using 2×2 strides (i.e., $i = 6$, $k = 3$, $s = 2$ and $p = 1$). It is equivalent to convolving a 3×3 kernel over a 2×2 input (with 1 zero inserted between inputs) padded with a 1×1 border of zeros (with an additional border of size 1 added to the top and right edges) using unit strides (i.e., $i' = 3$, $\tilde{i}' = 5$, $a = 1$, $k' = k$, $s' = 1$ and $p' = 1$).*
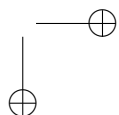
CHAPTER 6

State of the art
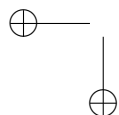
6.1 Introduction

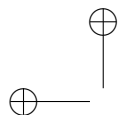Write something about SOTA in classification, detection, semantic segmentation, video segmentation
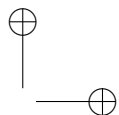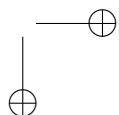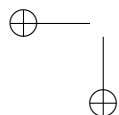
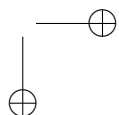CHAPTER 7
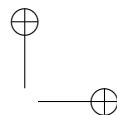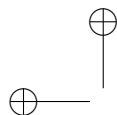
ReNet

7.1 Introduction
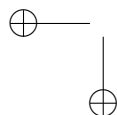
Write something about ReNet
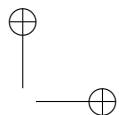
CHAPTER *8*

ReSeg

8.1 Introduction
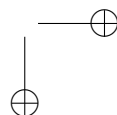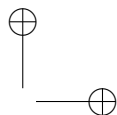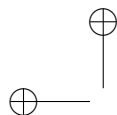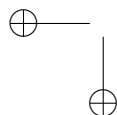
Write something about ReSeg

CHAPTER 9

DeconvRNN
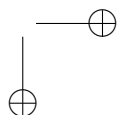
9.1 Introduction

Write something about video segmentation

Bibliography

Anonymous (2010). Deep sparse rectifier neural networks. Technical Report Anonymous, Anonymous. To appear.

Arpit, D., Zhou, Y., Kota, B. U., and Govindaraju, V. (2016). Normalization propagation: A parametric technique for removing internal covariate shift in deep networks. *arXiv preprint arXiv:1603.01431*.

Bengio, I. G. Y. and Courville, A. (2016). Deep learning. Book in preparation for MIT Press.

Bishop, C. M. (2006). *Pattern Recognition and Machine Learning*. Springer.

Boureau, Y., Bach, F., LeCun, Y., and Ponce, J. (2010a). Learning mid-level features for recognition. In *Proc. International Conference on Computer Vision and Pattern Recognition (CVPR'10)*. IEEE.

Boureau, Y., Ponce, J., and LeCun, Y. (2010b). A theoretical analysis of feature pooling in vision algorithms. In *Proc. International Conference on Machine learning (ICML'10)*.

Boureau, Y., Le Roux, N., Bach, F., Ponce, J., and LeCun, Y. (2011). Ask the locals: multi-way local pooling for image recognition. In *Proc. International Conference on Computer Vision (ICCV'11)*. IEEE.

Cooijmans, T., Ballas, N., Laurent, C., and Courville, A. (2016). Recurrent batch normalization. *arXiv preprint arXiv:1603.09025*.

Drachman, D. A. (2005). Do we have brain to spare? *Neurology*, **64**(12), 2004–2005.

Glorot, X., Bordes, A., and Bengio, Y. (2011). Deep sparse rectifier neural networks. In *AISTATS'2011*.

Hebb, D. O. (1949). *The Organization of Behavior*. Wiley, New York.

Im, D. J., Kim, C. D., Jiang, H., and Memisevic, R. (2016). Generating images with recurrent adversarial networks. *arXiv preprint arXiv:1602.05110*.

Bibliography

Ioffe, S. and Szegedy, C. (2015). Batch normalization: Accelerating deep network training by reducing internal covariate shift.

Jarrett, K., Kavukcuoglu, K., Ranzato, M., and LeCun, Y. (2009). What is the best multi-stage architecture for object recognition? In *ICCV'09*.

Krizhevsky, A., Sutskever, I., and Hinton, G. (2012a). ImageNet classification with deep convolutional neural networks. In *Advances in Neural Information Processing Systems 25 (NIPS'2012)*.

Krizhevsky, A., Sutskever, I., and Hinton, G. E. (2012b). Imagenet classification with deep convolutional neural networks. In *Advances in neural information processing systems*, pages 1097–1105.

Laurent, C., Pereyra, G., Brakel, P., Zhang, Y., and Bengio, Y. (2015). Batch normalized recurrent neural networks. *CoRR*, **abs/1510.01378**.

Le Cun, Y., Bottou, L., and Bengio, Y. (1997). Reading checks with multilayer graph transformer networks. In *Acoustics, Speech, and Signal Processing, 1997. ICASSP-97., 1997 IEEE International Conference on*, volume 1, pages 151–154. IEEE.

LeCun, Y., Bengio, Y., and Hinton, G. (2015). Deep learning. *Nature*, **521**, 436–444.

Linnainmaa, S. (1970). *The representation of the cumulative rounding error of an algorithm as a Taylor expansion of the local rounding errors.* Master's thesis, Univ. Helsinki.

Long, J., Shelhamer, E., and Darrell, T. (2015). Fully convolutional networks for semantic segmentation. In *Proceedings of the IEEE Conference on Computer Vision and Pattern Recognition*, pages 3431–3440.

McCulloch, W. S. and Pitts, W. (1943). A logical calculus of ideas immanent in nervous activity. **5**, 115–133.

Minsky, M. L. and Papert, S. A. (1969). *Perceptrons.* MIT Press, Cambridge.

Nair, V. and Hinton, G. E. (2010). Rectified linear units improve restricted Boltzmann machines. In *Proc. 27th International Conference on Machine Learning*.

Radford, A., Metz, L., and Chintala, S. (2015). Unsupervised representation learning with deep convolutional generative adversarial networks. *arXiv preprint arXiv:1511.06434*.

Rosenblatt, F. (1957). The perceptron — a perceiving and recognizing automaton. Technical Report 85-460-1, Cornell Aeronautical Laboratory, Ithaca, N.Y.

Rumelhart, D. E., Hinton, G. E., and Williams, R. J. (1986). Learning representations by back-propagating errors. *Nature*, **323**, 533–536.

Saxe, A., Koh, P. W., Chen, Z., Bhand, M., Suresh, B., and Ng, A. (2011). On random weights and unsupervised feature learning. In L. Getoor and T. Scheffer, editors, *Proceedings of the 28th International Conference on Machine Learning (ICML-11)*, ICML '11, pages 1089–1096, New York, NY, USA. ACM.

Visin, F., Kastner, K., Courville, A. C., Bengio, Y., Matteucci, M., and Cho, K. (2015). Reseg: A recurrent neural network for object segmentation.

Werbos, P. (1974). *Beyond Regression: New Tools for Prediction and Analysis in the Behavioral Sciences.* Ph.D. thesis, Harvard University.

Bibliography

Zeiler, M. D. and Fergus, R. (2014). Visualizing and understanding convolutional networks. In *Computer vision–ECCV 2014*, pages 818–833. Springer.

Zeiler, M. D., Taylor, G. W., and Fergus, R. (2011). Adaptive deconvolutional networks for mid and high level feature learning. In *Computer Vision (ICCV), 2011 IEEE International Conference on*, pages 2018–2025. IEEE.